



Behavior of Reinforced Concrete Columns Reinforced with GFRP Bars

Abeer M. Erfan ^a, Gamal T. Abd-Elrahman ^b, Youssef H. Hammad ^c, Mohamed Eissawy Ali^{d*}

^a Associate Professor, Ditto ; Abir.arfan@feng.bu.edu.eg.

^b Associate Professor, Faculty of Engineering (Shoubra), Benha Univeristy,Egypt ; gather@systra.ae

^c Professor, Faculty of Engineering (Shoubra), Benha Univeristy,Egypt ; a_youssef83@hotmail.com

^d Msc. Student, Ditto; eng_mohamedrc@yahoo.com

* Corresponding author

Abstract

Fiber composites as reinforcement gained a great acceptance in reinforcement different concrete elements. This is due to its high tensile strength and its performance in the concrete columns as longitudinal and transverse reinforcement stirrups. In this study Glass Fiber Reinforced Polymers (GFRP) with different diameters are applied. Four groups of concrete columns with fixed longitudinal reinforcement of 4 Φ 10 as main steel reinforcement and different transverse reinforcement in diameter and number (stirrups) were studied. First specimen was the control one reinforced with ordinary steel reinforcement the other specimens reinforced using GFRP stirrups different in diameter Φ 6, 8, 10 and the number of stirrups in meter. The transverse reinforcement effects the ultimate failure, local capacity, lateral deflection and ductility ratio.

The vertical displacement, cracking load and ultimate load of the tested columns were recorded and analyzed. The ultimate load increased. In first group, the ultimate load increased by 8.2%, 23.5% and 44.3% as the confinement numbers of GFRP stirrups increased from 575 kN to 622 kN to 710 kN to 830 kN. For second group, the ultimate load increased by 30.4%, 37.4% and 54.8% as the confinement numbers of GFRP stirrups increased from 575 kN to 750 kN to 790 kN to 890 kN. For third group, the ultimate load increased by 39.1%, 47.8% and 60% as the confinement numbers of GFRP stirrups increased from 575 kN to 800 kN to 850 kN to 920 kN. NLFEA analysis was carried out. Good agreement between the experimental and the NLFEA results was achieved.

Keywords : concrete columns, GFRP confinement, transverse reinforcement.

1. Introduction

Reinforced concrete buildings using Fiber-Reinforced Polymer (FRP) bars and, in particular, glass FRP (GFRP), has grown more widespread in recent decades. Corrosion-resistant GFRP bars have proven a major advantage over steel bars in many structural applications because of their resistance to corrosion, sea water, and other hostile conditions. Another benefit of GFRP bars is their excellent strength and low weight at a reasonable cost. Moreover, the use of longitudinal Glass Fiber-Reinforced Polymer (GFRP) bars in concrete structures has been reasonably well-established (Benmokrane et al. [1], Bischoff [2], El-Sayed et al. [3] and Nanni [4]). It's rare, but not impossible, to utilize longitudinal GFRP bars in concrete columns thus far. GFRP stirrups have been debated over whether or not they should be included in the computation of column capacity.

Fiber Reinforced Polymers (FRP) are being used in structural applications worldwide thanks to international norms and recommendations for their design, manufacturing, reinforcement, and quality control. FRP features may now be taken use of by designers thanks to the publication of the ECP 208 (2005) [5] standards. In spite of these design principles, more research is needed to better understand how GFRP-reinforced concrete columns function.

As reinforcement for diaphragm walls' soft eyes and waste water network manholes, Fiber Reinforced Polymers (FRP) bars have been employed in Egypt's underground metro stations recently. Efforts in Egypt to produce FRP bars of this kind are still in their infancy, and more work must be done in the form of new manufacturing methods and research.

In terms of linear elastic stiffness, FRP bars have a greater tensile strength than high-grade steel bars until brittle fracture. It is only in the direction of the fibers that the FRP reinforcement has significant tensile strength, making it an anisotropic material. The absence of material ductility must be taken into consideration while designing FRP reinforced concrete members because of the bars' linear elastic behavior without yielding. The most popular kind of FRP reinforcement (Glass FRP) has a lower stiffness than steel reinforcement, which must be taken into consideration in the ultimate and serviceability limit-state designs, as well as the influence on member deformations and crack width estimates.

FRP-reinforced geopolymer concrete (FRP-RC) Kassem et al. [6], steel-reinforced geopolymer concrete (S-RGC) Abraham et al. [7], and FRP-

reinforced geopolymer concrete (FRP-RC) systems have been studied extensively for their flexural and shear characteristics (FRP-RGC) Maranan et al. [8]. The behavior of compression members formed of these systems has been studied in comparatively few researches [8]. According to Paramanatham [9], compression stresses GFRP bars up to 20–30 percent of their maximum strength when tested on fourteen 200 mm by 200 mm by 1800-mm GFRP reinforced beam columns. Hognestad et al. [10] found that replacing the longitudinal steel bars with an equivalent quantity of GFRP bars decreased column capacity by 13 percent regardless of the tie type (steel or GFRP). The longitudinal GFRP bars provided 5–10% of the column capacity, according to the research done by De Luca et al. [11] and Tobbi et al. [12] on several square columns reinforced with GFRP bars and ties. According to the research done by Tobbi et al. [12] on several 350 mm by 350 mm concrete columns, it has been discovered that (1) GFRP bars can be used as compression members as long as there is enough confinement to prevent bar buckling, and (2) GFRP ties are effective at increasing the strength, toughness, and ductility of the confined concrete core. Pantelides et al. [13] conducted axial compression tests on two circular columns with GFRP spirals and vertical reinforcement. The axial load capacity of these columns was found to be 84% of that of control column, according to the findings of the tests. Circular columns reinforced with glass fiber reinforced polymer bars and ties were studied by Afifi et al. [14] and Mohamed et al [15]. According to their research, GFRP-RC columns behaved similarly to steel-RC columns, although on average, they were 7.0% less capable of supporting the same amount of weight. Because they are more cost-effective and lower in weight, these new columns may be used in lieu of traditional restricted concrete columns. In addition, since GFRP stirrups are inexpensive, the research sought to reduce manufacturing costs by using GFRP confined columns. Using non-metallic materials may also help constructions last longer. The effects of employing GFRP stirrups, the number of GFRP stirrups, the diameter of GFRP stirrups, and confinement in raising the axial compression stress are all examined in this research.

ANSYS 15 [16] was used to construct a nonlinear finite element model for columns with GFRP stirrups, which was used to simulate their behavior. The load-carrying capability of the columns was predicted using this model. Comparing the NLFEA findings with the experimental data will verify the model's validity.

2. EXPERIMENTAL PROGRAM

At the Housing and Building National Research Center, an experimental program was conducted to investigate the behavior of reinforced concrete columns reinforced with GFRP stirrups (HBNRC). Ten concrete columns, each with a unique reinforcing, make up this program. The ultimate capacity, concrete and GFRP stirrups stresses, fracture propagation, and the manner of failure of concrete columns are all being assessed.

2.1 Experimental Study

2.1.1 Concrete Mix

There was concrete mix design in the experimental program to get compressive strength of 35 MPa after 28 days. The concrete mix consists of different materials weights which presented in Table 1. There were six concrete cubes poured during the concrete columns casting as shown in Figure 1.

TABLE 1. Concrete Mixes, Materials Weights

Materials	$f_{cu} = 35 \text{ MPa}$	Units
Cement	400	Kg/m^3
Coarse aggregate	1040	Kg/m^3
Fine aggregate	550	Kg/m^3
Water	416	Kg/m^3
Super-plasticizer	11.63	Kg/m^3



FIGURE 1. Concrete cubes for examined columns.

2.1.2 GFRP Bars

GFRP bars were used as stirrups instead of steel reinforcement due to its ability for corrosion under different parameters. GFRP bars tensile strength is about 1.6 - 2.1 the tensile strength of reinforcing steel as shown in Figure 2.

In order to reduce the cost of the GFRP bars used in the experimental work, it was manufactured locally having skewers similar to

those commercially manufactured. The tensile strength of these bars varied between 600 MPa, 675 MPa and 750 MPa for diameters 6 mm, 8 mm and 10 mm respectively as shown in Table 2. These values were measured due to the pull-out test for these bars carried out in the National Building Research Center as shown in Figure 3.

TABLE 2. Tensile strength and ultimate strains of the used GFRP

Diameter (mm)	Tensile strength (MPa)	Ultimate strain (mm/mm)
6	600	0.0037
8	675	0.005
10	750	0.0049

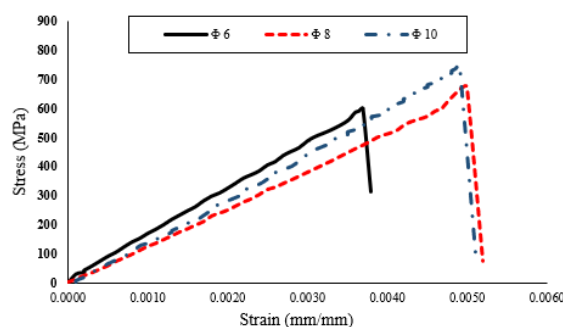


FIGURE 2. Stress-strain curve for the used GFRP bars.

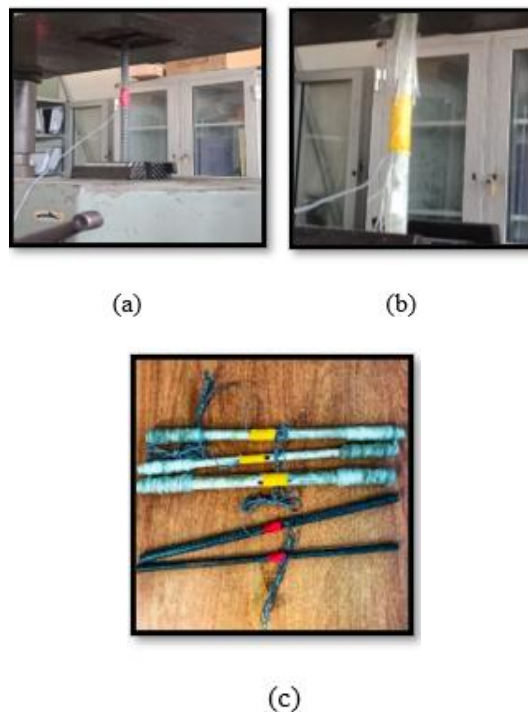


FIGURE 3. Tensile test of reinforcing bars, a) Steel bar; b) GFRP bar of Φ 10 mm; c) Different bars diameters Φ 6, 8 and 10 mm.

2.1.3 Steel Bars

Deformed high tensile steel bars of 10 mm diameter with yield strength of 400 MPa and ultimate strength of 520 MPa was used as main reinforcement for all specimens. Mild steel of 8 mm diameter with a yield strength of 240 MPa and ultimate strength of 360 MPa was used as stirrups for control specimen. The stress-strain relationship is given in Figure 4.

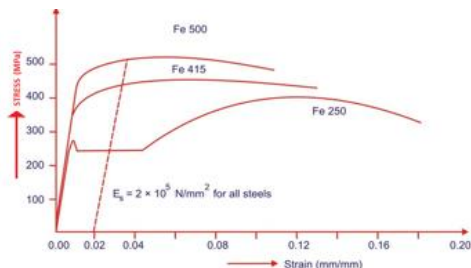


FIGURE 4. Typical stress-strain curves for steel.

2.1.4 Description of Concrete Columns

The experimental program consists of three groups of concrete columns in addition to the control specimen with dimensions 200 mm length, 200 mm width and 1200 mm height with 4 Φ 10 longitudinal steel reinforcement bars. All specimens has 35 MPa concrete compressive strength. Details of the experimental program are shown in Table 3 and Figure 5.

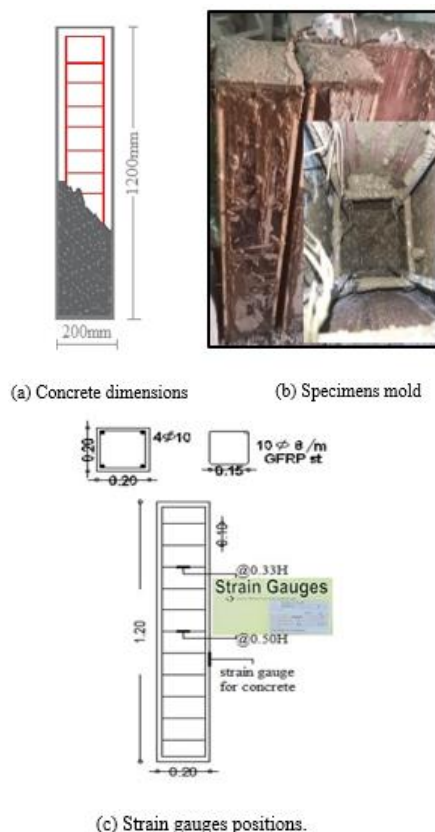


FIGURE 5. Specimens details.

TABLE 3. Specimens Details.

Specimen Group	Specimen Symbol	Longitudinal Steel Reinforcement	Stirrups Diameter. (mm)	Stirrups Numbers/m`	Stirrups Type
Control Sp. Group A	C _A	4 Φ 10	Ø8	7	Steel
Group B	C _{B-1}	4 Φ 10	Ø6	5	GFRP
	C _{B-2}	4 Φ 10	Ø6	7	GFRP
	C _{B-3}	4 Φ 10	Ø6	10	GFRP
Group C	C _{C-1}	4 Φ 10	Ø8	5	GFRP
	C _{C-2}	4 Φ 10	Ø8	7	GFRP
	C _{C-3}	4 Φ 10	Ø8	10	GFRP
Group D	C _{D-1}	4 Φ 10	Ø10	5	GFRP
	C _{D-2}	4 Φ 10	Ø10	7	GFRP
	C _{D-3}	4 Φ 10	Ø10	10	GFRP

2.1.5 Test Setup

The columns were tested under two-point load. Universal testing machine has maximum capacity of 5000 kN was used as shown in Figure 6. The load was incrementally applied to the specimen with rate

50 kN. Dial gauges with accuracy of 0.005 mm were used. Also, LVDTs were used to record the lateral and the vertical displacements every 0.5 kN increment of load. The load was increased until

failure and the load strains, displacements were recorded.

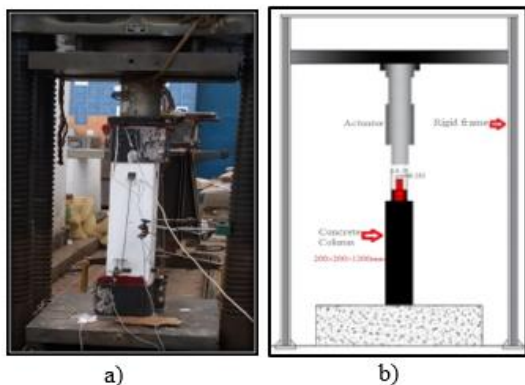


FIGURE 6. Test setup; a) Test machine; b) Schematic diagram for axial centric loading test.

3. EXPERIMENTAL RESULTS and DISCUSSION

The experimental results obtained from the experimental program are presented in terms of cracking load, ultimate load, mode of failure, effect of stirrups diameter, effect of stirrups number and displacement for each group of tested columns. This will be discussed in the following terms.

3.1 Cracking Load

The fractures in the control specimen begin at 240 kN at the column head, where the load is constant, and spread rapidly at 575 kN, when the load is increased to its maximum. Cracks appeared more slowly in the other groups that contains GFRP stirrups, as mentioned below.

For the second (group B), which utilized a different numbers of GFRP stirrups with diameter 6mm. When specimen CB-1 reached a failure load of 170 kN, the first crack appeared and continued to grow in the length and the breadth. There was 16.7% and 33.33% increase in the first crack load for specimens CB-2 and CB-3, respectively, compared to the control specimen. The fractures in specimen CC-1, utilized by group C and containing 8mm GFRP stirrups, began at a tension of 190 kN. The initial crack load was found to be decreased by 20.8%. There was an increase of 25% and 41.7 % in the initial crack load for CC-2 and CC-3 in comparison to the control specimen. Specimen CD-1 recorded a first crack load of 200 kN for group D specimens, and indicated a drop of 16.7 %. The measured first crack loads for specimens CD-2 and CD-3 were 320 kN and 370 kN, respectively, and increased by 33.3% and 54.2% in comparison to the control specimen, as shown in Table 4. GFRP stirrups improved the propagation and length of cracks.

TABLE 4. Cracking and Ultimate Loads of Tested Specimens.

Sp. Group	Sp. Symbol	Frist Crack Load (kN)	% of Decrease or Increase of Cracking Load Compared to CA	Ultimate Load (kN)	% of Decrease or Increase of Ultimate Load Compared to CA
Control Sp.	CA	240	0	575	0
Group B	CB-1	170	-29.2	622	8.2
	CB-2	280	16.7	710	23.5
	CB-3	320	33.3	830	44.3
Group C	CC-1	190	-20.8	750	30.4
	CC-2	300	25.0	790	37.4
	CC-3	340	41.7	890	54.8
Group D	CD-1	200	-16.7	800	39.1
	CD-2	320	33.3	850	47.8
	CD-3	370	54.2	920	60

3.2 Load

Control specimen, CA, failed at 575 kN for Group A, which was constrained by 8 mm steel stirrups (see Table 4). For Group B confined with 6 mm GFRP stirrups with different numbers, specimen CB-1 reinforced with 5 GFRP stirrups/m' showed an increase in ultimate load of 622 kN compared to

control specimen. The failure load was 710 kN for specimen CB-2 reinforced with 7 GFRP stirrups/m'. The failure load was 830 kN for specimen CB-3 reinforced with 10 GFRP stirrups/m'. Table 4 shows that the load-carrying capability of CB-1, CB-2, and CB-3 was improved by 8.2%, 23.5%, and 44.3%, respectively. There were 8 mm GFRP stirrups in Group C, and the first example was CC-1 reinforced with five stirrups. The failure load was 750 kN. The failure load was 790 kN for the GFRP stirrup-

reinforced C_{C-2} specimen. The failure load for the C_{C-3} specimen reinforced with 10/m' GFRP stirrups was 890 kN. According to Table 4, the load-carrying capacity of C_{C-1} , C_{C-2} , and C_{C-3} was increased by 30.4 percent, 37.4 percent, and 54.8 percent, respectively. There was a failure load of 800 kN for the specimen C_{D-1} reinforced with GFRP stirrups in Group D reinforced with ten mm of GFRP stirrups. An 850 kN failure load was applied to the GFRP stirrup-reinforced C_{D-2} specimen. Reinforced GFRP stirrups in the C_{D-3} specimen resulted in failure loads of 920 kN. According to the data given in Table 4, the increase in carrying capacity for C_{D-1} , $CD-2$, and $CD-3$ was 39.1%; 47.8%; and 60%. Table 4 showed that all specimens had a higher ultimate load compared to the Control Specimen. As a consequence of the confinement effect created by varying the diameter and spacing of GFRP stirrups, this increase is not constant.

3.3 Modes of Failure

The control specimen collapsed in a compression failure mode followed by local concrete crushing and spalling on the column's surface. Loads reached their maximum near failure and then fell by 70% to 50% of the maximum load with increasing the descending section of load displacement curves compared to the failure mode for the other tested specimens. These specimens become more ductile and absorb more energy.

3.4 Effect of Stirrups Diameter

A comparison between the specimens which used the same numbers of GFRP stirrups with different diameter was done. Cracks propagation in control specimen C_A started at the column head at load 240 kN at the point of load concentration, then it propagates suddenly at the maximum load of 575 kN and after this the load decreases and the cracks increased with the loading rate, showing the failure of column. For specimens which used 5 GFRP stirrups/m` with different diameters (C_{B-1} with Φ 6 GFRP stirrups, C_{C-1} with Φ 8 GFRP stirrups, and C_{D-1} with Φ 10 GFRP stirrups) different values of cracking load were recorded which represents decrease of 29.2%, 20.8% and 16.7% respectively with respect to the control specimen. The ultimate load of the same specimens were recorded to show an increase in the failure load of 8.2%, 30.4% and 39.1% respectively with respect to the control specimen as shown in Figure 7a. For specimens which used 7 GFRP stirrups/m` with different diameter (C_{B-2} with Φ 6 GFRP stirrups, C_{C-2} with Φ 8 GFRP stirrups, and C_{D-2} with Φ 10 GFRP stirrups)

the recorded cracking load showed an increase about 16.7%, 25% and 33.33% respectively with respect to the control specimen. Also, the recorded ultimate load showed an increase about 23.5%, 37.4% and 47.8% respectively with respect to the control specimen as shown in Figure 7b. For specimens which used 10 GFRP stirrups/m` with different diameter (C_{B-3} with Φ 6 GFRP stirrups, C_{C-3} with Φ 8 GFRP stirrups, and C_{D-3} with Φ 10 GFRP stirrups) different values of cracking load were recorded to show the increase of 33.33%, 41.7%, and 54.2% respectively with respect to the control specimen. Also, the recorded ultimate load showed an increase about 44.3%, 54.8% and 60% respectively with respect to the control specimen as shown in Figure 7c. It was clear that, using 10 Φ 10/m` GFRP stirrups is the most effective in increasing the load-carrying capacity of the column by 60% compared to the other diameters of GFRP stirrups.

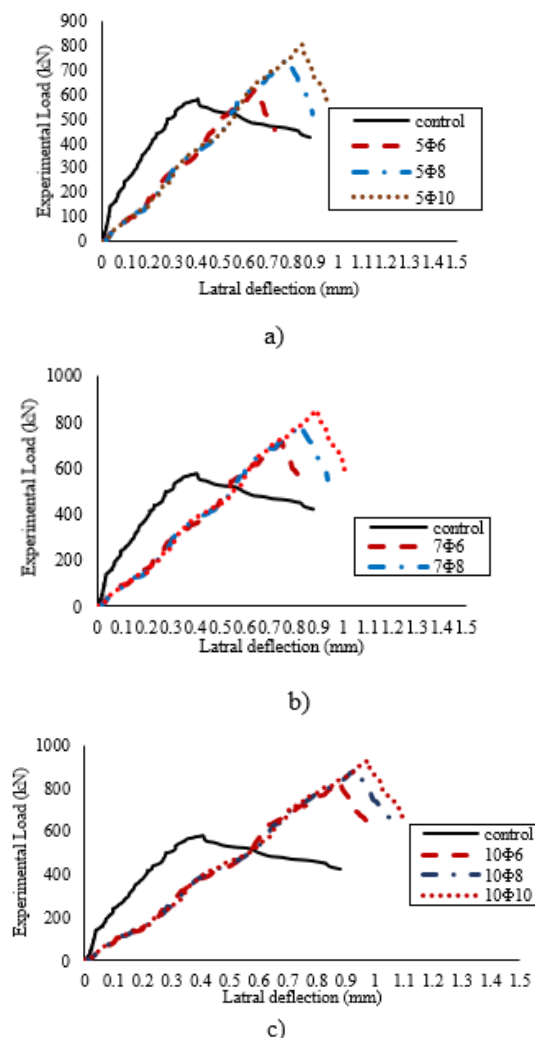


FIGURE 7. Effect of stirrups diameter on load-displacement response; a) Stirrups spacing 200 mm; b) Stirrups spacing 140 mm; c) Stirrups Spacing 100 mm.

3.5 Effect of Stirrups Numbers

A comparison between the specimens which used the same diameters of GFRP stirrups with different number was done. It has been noticed that the cracks propagation in control specimen CA started at the column head at load 240 kN at the point of load concentration, then it propagated suddenly at the maximum load of 575 kN, after this the load decreased and the cracks increased with the loading rate, showing the failure of column. For specimens have Φ 6 GFRP stirrups with different numbers (CB-1 with 5 /m` GFRP stirrups, CB-2 with 7 /m` GFRP stirrups and CB-3 with 10 /m` GFRP stirrups) the recorded cracking load for CB-1 decrease about 29.2% and increase for CB-2, and CB-3 about 16.7%, 33.3% respectively with respect to control specimen. For the ultimate load of the same previous specimens were recorded an increase of 8.2%, 23.5% and 44.3% respectively with respect to control specimen as shown in Figure 8a. For specimens which has Φ 8 GFRP stirrups with different number (CC-1 with 5 /m` GFRP stirrups, CC-2 with 7 /m` GFRP stirrups and CC-3 with 10 /m` GFRP stirrups) different values of cracking load were recorded. The decrease for CC-1 was 20.8% and the increase for CC-2, and CC-3 was 25% and 41.7% with respect to the control specimen. Also, the recorded ultimate load showed an increase about 30.4%, 37.4% and 54.8% respectively with respect to the control specimen as shown in Figure 8b. For specimens have Φ 10 GFRP stirrups with different number (CD-1 with 5 /m` GFRP stirrups, CD-2 with 7 /m` GFRP stirrups and CD-3 with 10 /m` GFRP stirrups) different values of cracking load were recorded. The decrease for CD-1 was 16.7% and the increase for CD-2, and CD-3 of 33.3%, 54.2% respectively with respect to the control specimen. Also, the recorded ultimate load showed an increase about 39.1%, 47.8% and 60% respectively with respect to the control specimen as shown in Figure 8c. It was clear that using the GFRP stirrups of 10 Φ 10/m` was the most effective in increasing the load-carrying capacity of the column by 60% with respect to the other spacing of GFRP stirrups in all groups. The ultimate load increased in all specimens with respect to the control specimen. The maximum value of the ultimate load belonged to small spacing in every group.

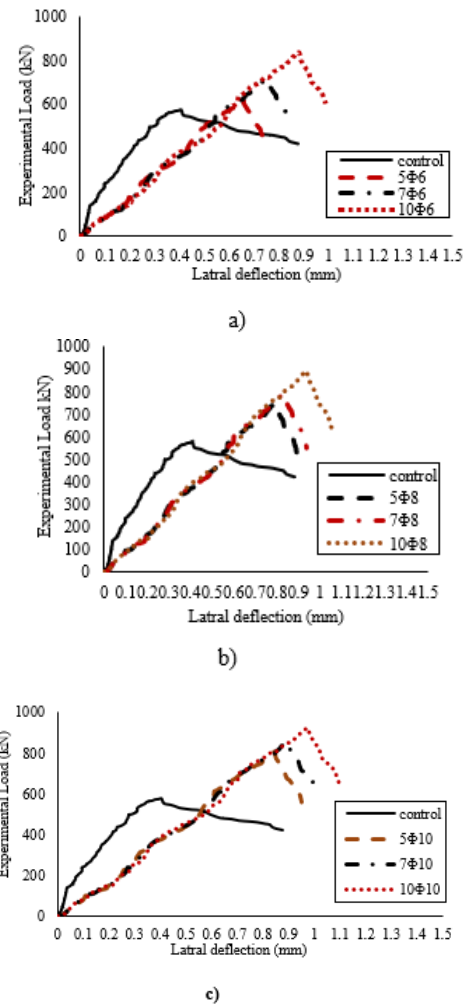


FIGURE 8. Effect of stirrups spacing on load-displacement response: a) Φ 6 mm; b) Φ 8 mm; c) Φ 10 mm.

3.6 Lateral Displacement

Firstly, loading may cause significant deformations. These deformations were represented by horizontal lateral displacements in x-direction. Displacement of Control Specimen was 0.45 mm at 575 kN failure load. Displacement of other Specimens were increased gradually with increasing of failure load with respect to Control Specimen. Table 5 and Figure 9 showing the lateral displacements.

TABLE 5. Vertical and Lateral Displacements of the Tested Specimens.

Specimen Group	Specimen Symbol	Failure Load (kN)	Lateral Displacement (mm)	Vertical Displacement (mm)	Enhancement % of Displacements Compared to CA	
					Lateral	Vertical

Control Sp. (Group A)	C _A	575	0.45	0.62	0	0
Group B	C _{B-1}	622	0.59	0.51	31.11	-17.74
	C _{B-2}	710	0.68	0.63	51.11	1.61
	C _{B-3}	830	0.79	0.61	75.56	-1.61
Group C	C _{C-1}	750	0.72	0.55	60.00	-11.29
	C _{C-2}	790	0.75	0.62	66.67	0.00
	C _{C-3}	890	0.84	0.63	86.67	1.61
Group D	C _{D-1}	800	0.77	0.59	71.11	-4.84
	C _{D-2}	850	0.82	0.51	82.22	-17.74
	C _{D-3}	920	0.88	0.49	95.56	-20.97

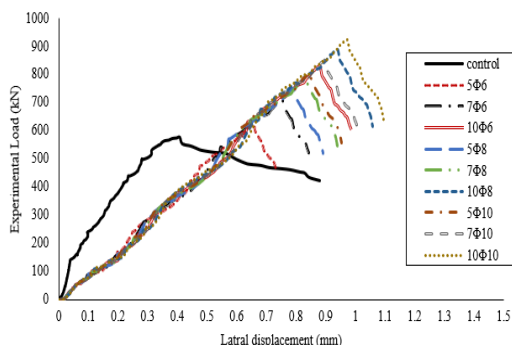


FIGURE 9. Comparison between Lateral Displacements of Specimens

3.7 Vertical Displacement

The deformations represented by vertical displacement were due to the applied loads which differ in each specimen. Displacement of Control Specimen was 0.62 mm at load of 575 kN. Displacement of other Specimens were very close to each other. Table 5 and Figure 10 show the vertical displacements.

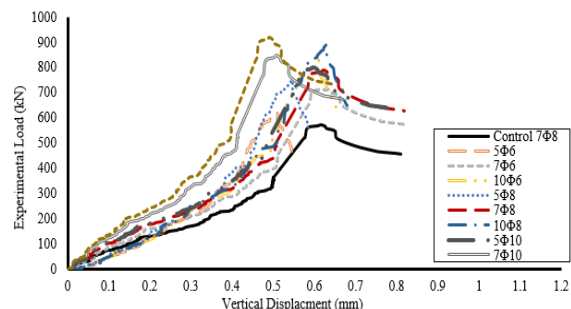


FIGURE 10. Load-vertical displacement for all specimens

4. NONLINEAR FINITE ELEMENT ANALYSIS of TEST SPECIMENS

The non-linear finite element approach using ANSYS 15 was applied to the tested columns to examine reliability of the approach in predicting the

behaviour of the reinforced concrete columns provided with GFRP stirrups. Typical modelling of the column elements representing the concrete and reinforcement is indicated in Figure 11. The NLFE predictions including cracking, ultimate loads, and maximum deflections, as compared to the experimental results are summarized in Table 6. In this investigation, the column models used solid 65 for representing the concrete elements and link 180 for the longitudinal bars and stirrups.

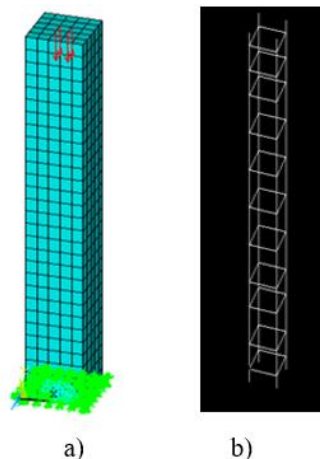


FIGURE 11. Typical modelling of the column elements: a) Concrete core of column; b) Typical reinforcement of column.

4.1 Crack Patterns

The cracking was initiated at early loading stage in the concrete elements modelling the loaded face of the column as shown in Figure 12. Referring to Table 6, the cracking capacity is shown to be 100 kN for all the specimens being independent on the reinforcing characteristics. The cracking load, as such, is quite below the experimental cracking capacity. The ratio of the numerical cracking load to the experimental load, P_{cr} (NLFE) / P_{cr} (EXP.) is shown to be ranged from 0.27 to 0.58 with a mean value of 0.39. This is

may be justified as the NLFE predictions represent the micro-cracking stage which precedes the visible cracking stage as shown in Table 6. On the other hand, the cracking patterns at each load increment revealed that propagation of the cracks for all specimens was slightly different with respect to the experimental cracking patterns. This reflects the potential of the nonlinear finite element analysis in determining the cracks propagation, and in assessing the significance of the reinforcing method on the cracking patterns as shown in Table 6.

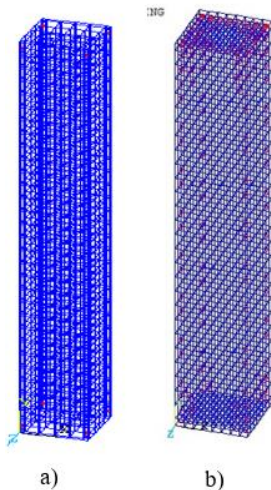


FIGURE 12. Control Specimen CA: a) Initial cracking at load of 100 kN; b) Crack pattern at failure

4.2 NLFEA Ultimate load

The analysis reflected the confinement significance. The numerical ultimate load capacity P_u for control specimen was 500 kN. The numerical ultimate load capacity P_u was as the following: For group B, the ultimate load capacity P_u was 497.6 kN, 605 kN, and 705 kN for Specimens CB-1, CB-2 and CB-3, respectively. The enhancement was 0%, 21%, 41% respectively. For group C, the ultimate load capacity P_u was 630 kN, 650 kN, and 739 kN for specimens CC-1, CC-2 and CC-3, respectively. The predicted enhancement was 26%, 30% and 47.8% for, respectively. For group D, the ultimate load capacity P_u was 680 kN, 748 kN, and 800 kN for specimens CD-1, CD-2 and CD-3, respectively. The numerical enhancement for was 36%, 49.6% and 60% as shown in Table 6.

4.3 NLFEA Displacement

In general, vertical displacement obtained from NLFEA were acceptable. Near failure, the maximum vertical displacement of the control specimen; CA

was equal to 0.53 mm. For Group B the vertical displacements were 0.41 mm, 0.53 mm and 0.52 mm for CB-1, CB-2 and CB-3 respectively. On the other hand, the numerical vertical displacements of group C were 0.46 mm, 0.51 mm and 0.52 mm for CC-1, CC-2 and CC-3 respectively. For group D, the predicted NLFE vertical displacements were 0.51 mm, 0.45 mm and 0.42 mm for CD-1, CD-2 and CD-3 respectively.

5. COMPARISON BETWEEN EXPERIMENTAL and NLFEA RESULTS

5.1 Ultimate load

Good agreement between the NLFEA predictions and the recorded load-carrying capacities as shown in Figure 13 for the control specimen. The average of NLFE load to the experimental load; P_u (NLFE) / P_u (EXP.) equal 0.86. For specimens in groups B, C and D the ratio of the numerical load to the experimental load; P_u (NLFE) / P_u (EXP.) ranges between 0.80 and 0.88 with a mean value of 0.86, as shown in Table 6. Furthermore, the analysis reflected the confinement significance. The enhancement in the ultimate load capacity P_u was as the following: For group B, the enhancement was 0%, 21%, and 41% for specimens CB-1, CB-2 and CB-3 compared to the experimental enhancement of 8.2%, 23.5% and 44.3% respectively. For group C, the predicted enhancement was 26%, 30% and 47.8% for CC-1, CC-2 and CC-3, respectively compared to the experimental enhancement of 30.4%, 37.4% and 54.8%, respectively. For group D the enhancement for CD-1, CD-2, and CD-3 was 36%, 49.6% and 60% compared to 39.1%, 47.8% and 60% of the experimental as shown in Fig. 14 to Fig. 17. In general, the NLFA predictions are shown to be slightly less than the experimental results being conservative in assessing the effect of increasing the lateral reinforcement on the load-carrying capacity of the column.

5.2 Vertical Displacement and Deformations

In general, vertical displacement obtained from NLFEA were agreed with the experimental results. Near failure, the maximum vertical displacement in the column for the control specimen; CA was equals to 0.53 mm. For group B the vertical displacement ranged between 0.41 mm and 0.53 mm being comparable to the recorded vertical displacements in the test which ranged between 0.51 mm and 0.63 mm. The ratios between the vertical displacement in

this group and the control specimen were 0.77 mm to 1.00 mm. On the other hand, the numerical vertical displacements in group C were varied between 0.46 mm and 0.52 mm. These values varied between 0.86 mm and 0.98 mm of control specimen. For group D, the predicted NLFE vertical displacements are 0.51 mm, 0.45 mm and 0.53 mm for CD-1, CD-2 and CD-3. The ratios between these values and that of the

control specimen are 0.96, 0.85 and 1.00. By studying these results, it is noticed that there was a good enhancement in different groups by using GFRP stirrups for confinement with respect to using steel stirrups in control specimen. The vertical displacement results at failure revealed the observed crushing of the concrete as shown in Fig. 14 to Fig. 17.

TABLE 6. Comparisons between NLFEA and experimental results

Specimen group	Spec. ID.	Experimental load (kN)		Numerical load (kN)		Δ (mm)		$\frac{P_u(NLFE)}{P_u(Exp)}$		$\frac{\Delta(NLFE)}{\Delta(Exp)}$
		Frist Crack	Max. Load	Frist Crack	Max. Load	Δ_{exp}	Δ_{NLFE}	Frist Crack	Max. Load	
Control	C _A	240	575	100	500.0	0.62	0.53	0.41	0.86	0.86
Group B	C _{B-1}	170	622	100	497.6	0.51	0.41	0.58	0.8	0.8
	C _{B-2}	280	710	100	605.0	0.63	0.53	0.35	0.85	0.85
	C _{B-3}	320	830	100	705.0	0.61	0.52	0.31	0.85	0.85
Group C	C _{C-1}	190	750	100	630.0	0.55	0.46	0.52	0.84	0.84
	C _{C-2}	300	790	100	650.0	0.62	0.51	0.33	0.82	0.82
	C _{C-3}	340	890	100	739.0	0.63	0.52	0.29	0.83	0.83
Group D	C _{D-1}	200	800	100	680.0	0.59	0.51	0.5	0.85	0.85
	C _{D-2}	320	850	100	748.0	0.51	0.45	0.31	0.88	0.88
	C _{D-3}	370	920.0	100	800.0	0.59	0.42	0.27	0.87	0.87
Average								0.387	0.86	0.86
Variance								0.011	0.00056	0.00056
Standard Deviation								0.109	0.024	0.024

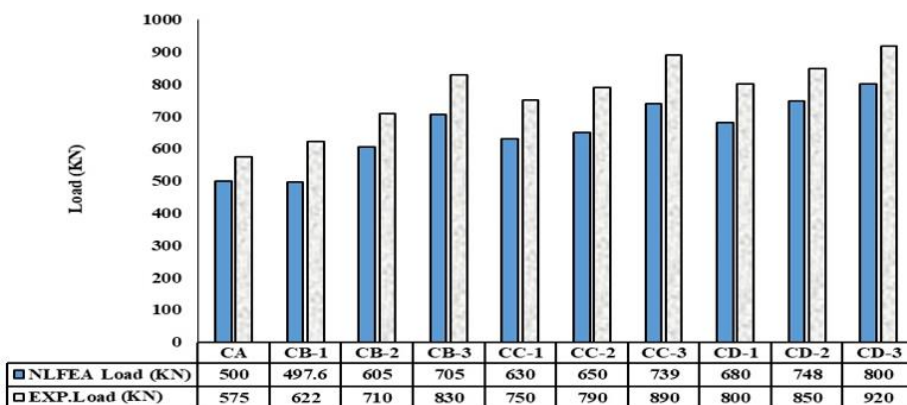
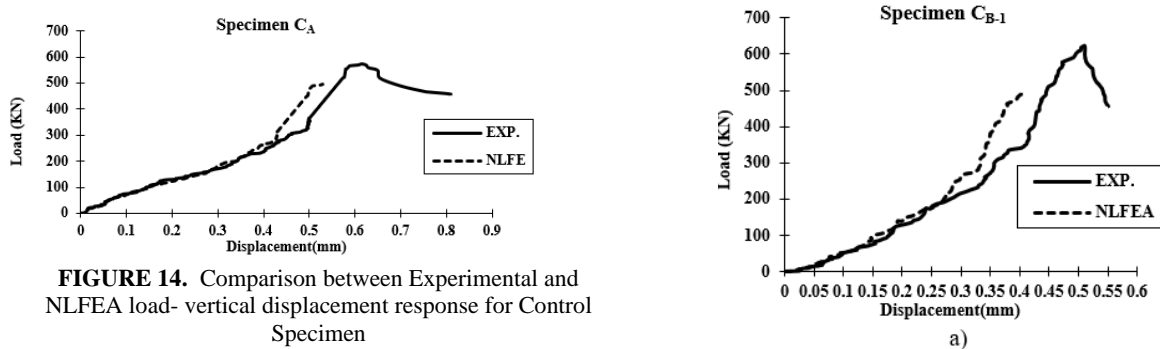
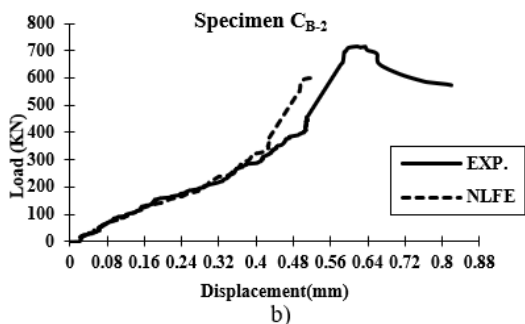
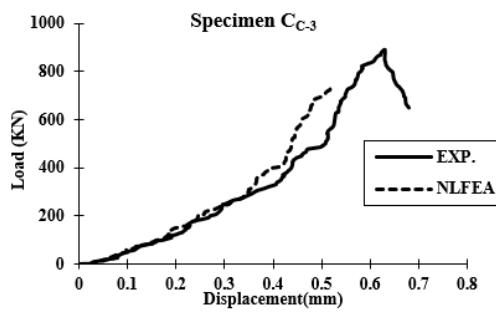


FIGURE 13. Comparison between Experimental and NLFEA Failure load.

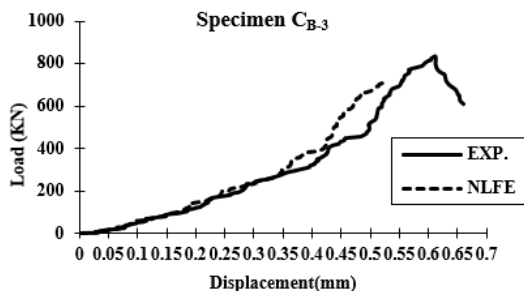




b)



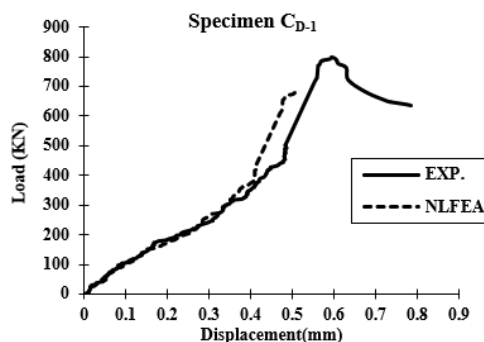
c)



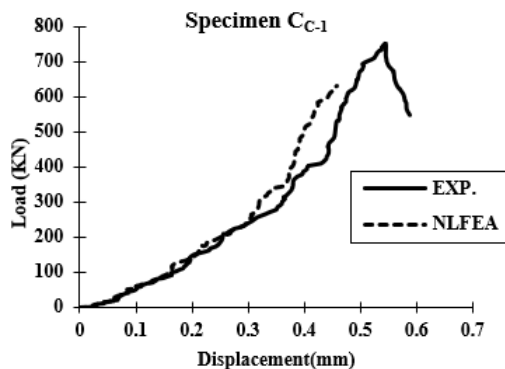
c)

FIGURE 15. Comparison between Experimental and NLFEA load- vertical displacement response for Group B; a) CB-1; b) CB-2; c) CB-3.

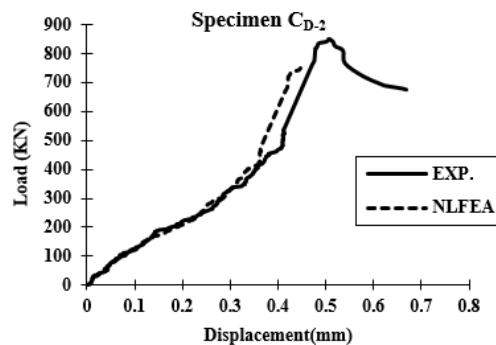
FIGURE 16. Comparison between Experimental and NLFEA load- vertical displacement response for Group C; a) Cc-1; b) Cc-2; c) Cc-3.



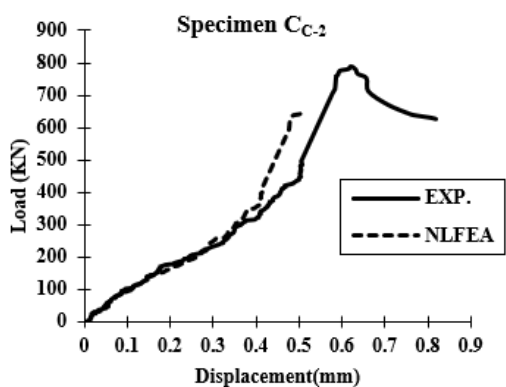
a)



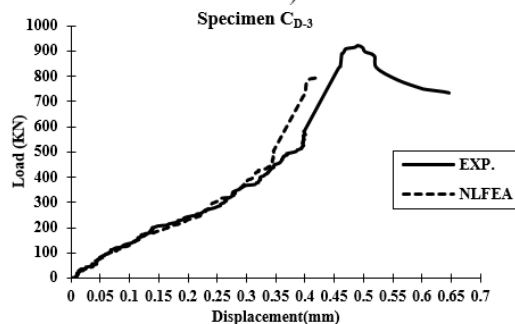
a)



b)



b)



c)

FIGURE 17. Comparison between Experimental and NLFEA load- vertical displacement response for Group D; a) CD-1; b) CD-2; c) CD-3.

5.3 Lateral Displacement

In general, lateral displacement obtained from NLFEA were agreed with the experimental results. Near failure, the maximum lateral displacement in the column for the control specimen; CA was equals to 0.41 mm in x-direction and 0.43 mm in y-direction. For group B in x-direction, the lateral displacement ranged between 0.22 mm to 0.28 mm being comparable to the recorded lateral displacements in the test which ranged between 0.28 mm and 0.33 mm. For group B in y-direction, the lateral displacement ranged between 0.21 mm to 0.27 mm being comparable to the recorded lateral displacements in the test which ranged between 0.26 mm and 0.32 mm. On the other hand, the numerical lateral displacements in group C were varied between 0.46 mm and 0.52 mm. These values varied between 0.25 mm and 0.28 mm in x-direction and between 0.24 mm to 0.27 mm in y-direction. For group D, the predicted NLFE lateral displacements in x-direction are 0.33 mm, 0.29 mm and 0.28 mm for CD-1, CD-2 and CD-3 and lateral displacements in y-direction are 0.35 mm, 0.31 mm and 0.29 mm as shown in figure 18 to figure 24.

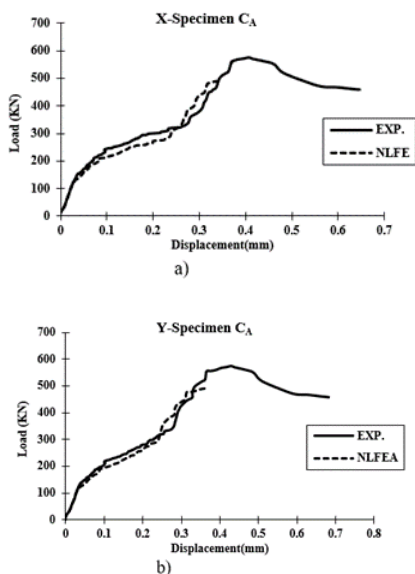


FIGURE 18. Comparison between Experimental and NLFEA load-lateral displacement response for Control Specimen: a) X-direction; b) Y-direction.

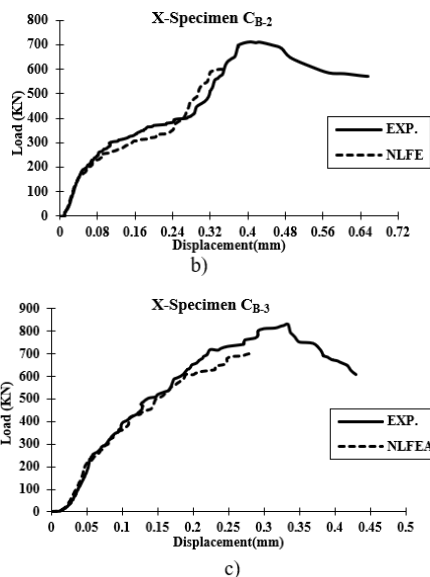
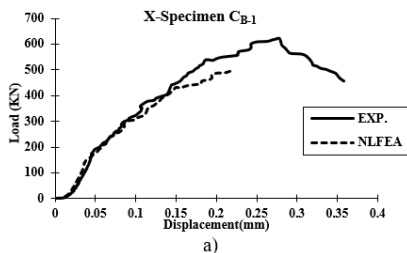


FIGURE 19. Comparison between Experimental and NLFEA load-lateral displacement response for Group B in x-direction; a) CB-1; b) CB-2; c) CB-3.

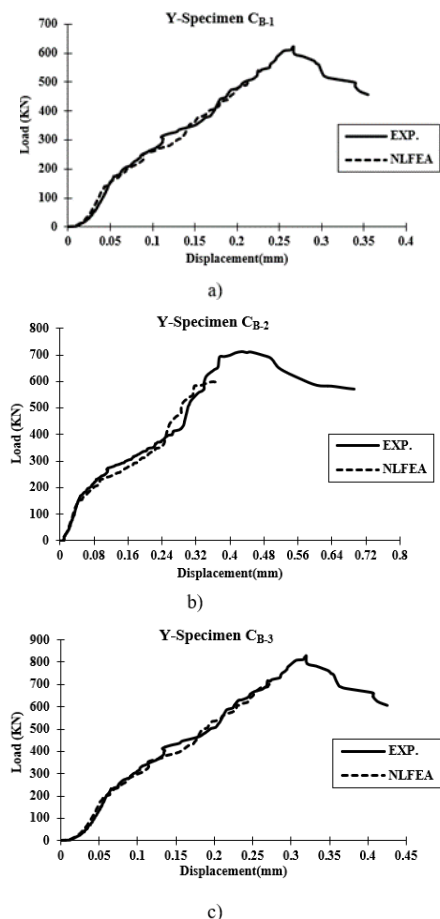


FIGURE 20. Comparison between Experimental and NLFEA load-lateral displacement response for Group B in y-direction; a) CB-1; b) CB-2; c) CB-3

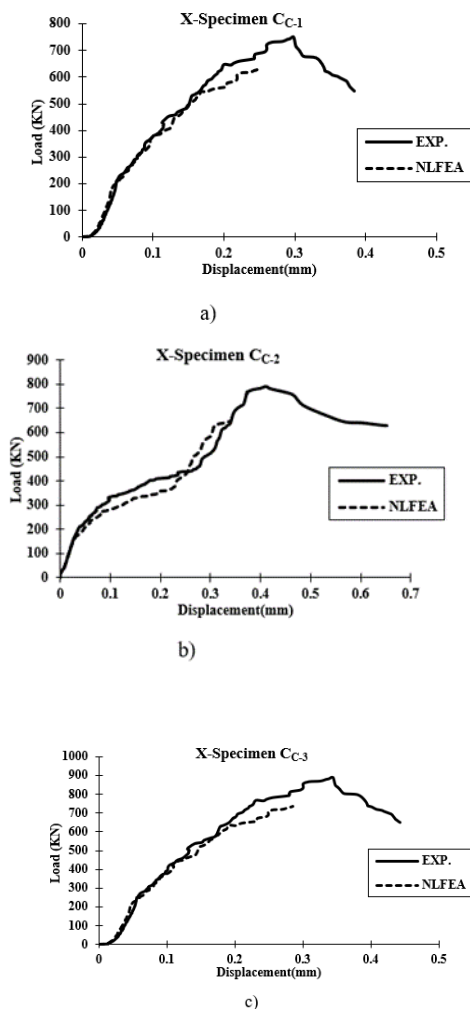


FIGURE 21. Comparison between Experimental and NLFEA load-lateral displacement response for Group C in x-direction; a) Cc-1; b) Cc-2; c) Cc-3.

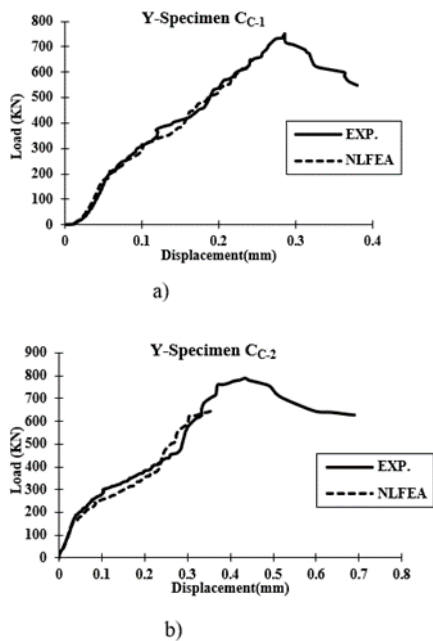


FIGURE 22. Comparison between Experimental and NLFEA load-lateral displacement response for Group C in y-direction; a) Cc-1; b) Cc-2; c) Cc-3.

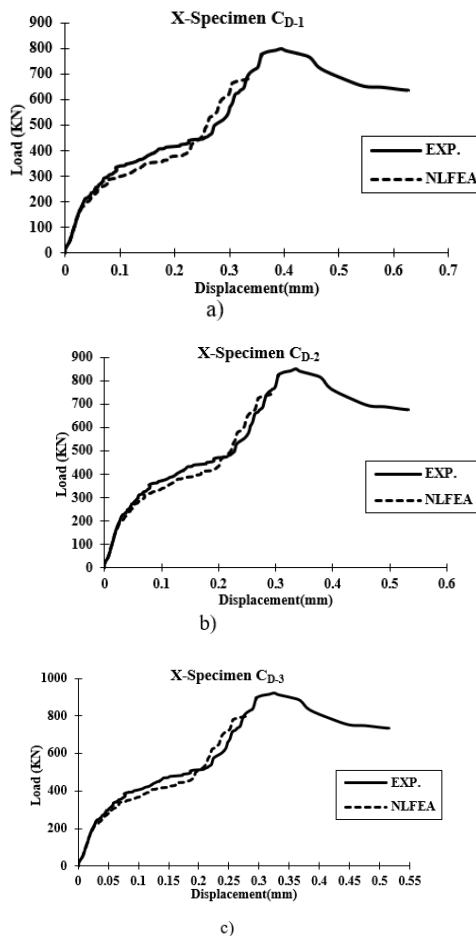
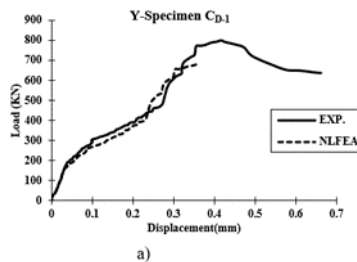


FIGURE 23. Comparison between Experimental and NLFEA load-lateral displacement response for Group D in x-direction; a) CD-1; b) CD-2; c) CD-3.



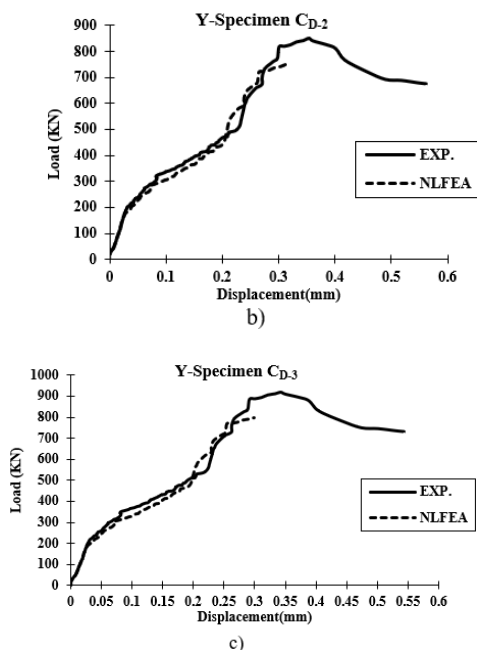


FIGURE 24. Comparison between Experimental and NLFEA load-lateral displacement response for Group D in y-direction; a) CD-1; b) CD-2; c) CD-3.

6. CONCLUSION

Conclusions may be derived from this study's experimental and numerical findings, which are detailed in this paper:

- 1- When subjected to axial compression, GFRP stirrups restricted specimens show better ultimate loads compared to the control specimen.
- 2- When the failure load is primarily dictated by the spalling of the mortar cover surrounding the main steel reinforcement, reducing the stirrups volume fraction has little impact.
- 3- Under compression pressure, increasing the number of GFRP stirrups has a significant impact on ultimate loads. When compared to a control specimen constrained with steel stirrups, specimens with the highest number and diameter (specimen CD-3) show a 60 percent increase in strength.
- 4- The test findings demonstrate that increasing the number and diameter of confining GFRP stirrups steadily increases the ultimate load. Because GFRP stirrups have fewer and smaller diameters than steel stirrups, they have a greater effect on the specimen's strength.
- 5- Due to its superior enhanced strength, an increase in stirrups volume fraction % outperformed a control specimen restrained

by steel stirrups reinforcement in delaying crack development.

- 6- Further parametric investigations using multiple parameters may benefit from the high degree of agreement between experimental and numerical findings.

7. ACKNOWLEDGEMENTS

A special thank goes out to the staff at the Reinforced Concrete Laboratory of Housing and Building National Research Centre (HBNRC) for their patience, perseverance, and excellent specimen installation.

8. REFERENCES

- [1] Benmokrane, B., Chaallal, O. and Masmoudi, R., 1995. Glass fibre reinforced plastic (GFRP) rebars for concrete structures. *Construction and Building Materials*, 9(6), 353-364.
- [2] Bischoff, P.H., 2005. Re-evaluation of deflection prediction for concrete beams reinforced with steel and fiber reinforced polymer bars. *Journal of Structural Engineering*, 131(5), pp.752- 767.
- [3] El-Sayed, A., El-Salakawy, E. and Benmokrane, B., 2005. Shear strength of one-way concrete slabs reinforced with fiber-reinforced polymer composite bars. *Journal of Composites for Construction*, 9(2), pp.147-157.
- [4] Nanni, A., 1993. Flexural behaviour and design of RC members using FRP reinforcement. *Journal of Structural Engineering*, 119(11), pp.3344-3359.
- [5] ECP 208 (2005), "Egyptian code of practice for design principles of the use of fiber-reinforced polymers in construction", permanent committee, code no. 208, issued 2005.
- [6] Kassem, C., Farghaly, A.S., Benmokrane, B. Evaluation of flexural behaviour and serviceability performance of concrete beams reinforced with FRP bars. *ASCE Journal Composite Construction* 2011; 15:682–95.
- [7] Abraham, R., Raj, S.D., Abraham, V. Strength and behaviour of geopolymer concrete beams. *International Journal*

- Innovative Research Science, Engineering Technoloe 2013;2:159–66.
- [8] Maranan, G., Manalo, A., Benmokrane, B., Karunasena, W., and Mendis, P. Evaluation of the flexural strength and serviceability of geopolymer concrete beams reinforced with glass-fibre-reinforced polymer (GFRP) bars. *Engineering Structures* 2015; 101:529–41.
- [9] Paramanatham, N, S. Investigation of the behaviour of concrete columns reinforced with fiber reinforced plastic rebars .M.Sc. thesis. Texas, USA: Lamar University; 1993.
- [10] Hognestad, L. Al Sayed, S, Al-Salloum, Y., Almusallam, T., and Amjad, M. Concrete columns reinforced by glass fiber reinforced polymer rods. *ACI Special Publication* 1999;188.
- [11] De Luca, A., Matta, F. and Nanni, A. 2010. Behavior of full-scale glass fiber-reinforced polymer reinforced concrete columns under axial load. *ACI Structural Journal*, 107(5): 589-596.
- [12] Tobbi, H., Farghaly, A.S. and Benmokrane, B. 2012. Concrete columns reinforced longitudinally and transversally with glass fiber-reinforced polymer bars. *ACI Structural Journal*, 109(4): 551-558.
- [13] Pantelides, C.P., Gibbons, M.E. and Reaveley, L.D., 2013. Axial load behaviour of concrete columns confined with GFRP spirals. *Journal of Composites for Construction*, 17(3), pp.305- 313.
- [14] Afifi, M.Z., Mohamed, H.M. and Benmokrane, B., 2013. Axial capacity of circular concrete columns reinforced with GFRP bars and spirals. *Journal of Composites for Construction*, 18(1), p.04013017.
- [15] Mohamed, H.M, Afifi, M, Z, and Benmokrane, B. Performance evaluation of concrete columns reinforced longitudinally with FRP bars and confined with FRP hoops and spirals under axial load. *Journal of Bridge Engineering* 2014; 19:04014020.